Quantized current in carbon nanotube quantum dots by surface acoustic waves

To cite this article: C Würstle *et al* 2007 *New J. Phys.* **9** 73

View the article online for updates and enhancements.

Related content

- Charge pumping and current quantization in SAW-driven carbon nanotube devices
  M R Buitelaar, P J Leek, V I Talyanskii et al.

- Acoustic charge transport in GaN nanowires
  J Ebbecke, S Maisch, A Wixforth et al.

- Fabrication and characterization of GaAs/AlGaAs lateral quantum dot
  Q-Z Yang, G A C Jones, M J Kelly et al.

Recent citations

- Transporting and manipulating single electrons in surface-acoustic-wave minima
  Christopher J. B. Ford

- Effect of periodic potential on exciton states in semiconductor carbon nanotubes
  Oleksiy Roslyak and Andrei Piryatinski

- Non-adiabatic quantized charge pumping with tunable-barrier quantum dots: a review of current progress
  Bernd Kaestner and Vyacheslavs Kashcheyevs

Quantized current in carbon nanotube quantum dots by surface acoustic waves

C Würstle[1], J Ebbecke[1,2,3], M E Regler[1] and A Wixforth[1,2]

[1] Institut für Physik der Universität Augsburg, Experimentalphysik I,
Universitätsstr. 1, 86159 Augsburg, Germany
[2] Center for NanoScience (CeNS), Geschwister-Scholl-Platz 1,
80539 Munich, Germany
E-mail: jens.ebbecke@physik.uni-augsburg.de

Abstract. Single charge effects attract much attention with respect to possible applications as future transistor structures or for quantum cryptography. Here, surface acoustic wave mediated single charge transport through quantum dots (QDs) formed in a carbon nanotube (CNT) is presented. The CNT bridges metallic source and drain contacts on a piezoelectric host substrate, employing an acoustic alignment technique. The metal electrodes in contact with the nanotube provide tunnel barriers to the quasi one-dimensional electron system, hence forming a few QD in series due to the presence of defects within the CNT. The dynamic piezoelectric field associated with the surface wave leads to an acoustoelectric current through the system which turns out to be quantized like in a turnstile device.

[3] Author to whom any correspondence should be addressed.

IOP Institute of Physics ⏀ DEUTSCHE PHYSIKALISCHE GESELLSCHAFT

Contents

1. Introduction

Low dimensional electron systems have become increasingly important in modern physics and technology. On one side, the semiconductor technology is rapidly advancing resulting in low dimensional effects even for industrial applications. On the other hand, the prosecution of this route by further miniaturization becomes increasingly difficult. Therefore alternative approaches have been devised by scientists all over the world. One such approach relies on self organization processes. Another possibility is to replace the lithographically defined artificial 'wiring' on a chip by natural systems with a high aspect ratio. If the diameter of these systems reaches the nanometre scale, one dimensional (1D) behaviour is expected to occur. In 1991, while investigating the properties of carbon, Iijima [1] discovered a novel manifestation of graphite, the so-called carbon nanotubes (CNTs). It turned out that they represent a natural ideal 1D conductor. Depending on the helicity, CNTs can exhibit metallic or semiconducting properties, making them even more interesting for potential applications. Moreover, apart from their electronic properties, they also show remarkable optical and mechanical properties, which triggered intensive research over the last two decades.

Electrical transport measurements through CNTs have already been made in the early years after their discovery. Moreover, different types of transistors employing CNTs have been demonstrated in the recent past. If a CNT is contacted by metal contacts, potential barriers form at the metal–CNT interface. If the distance between both metal contacts is short enough, such that the separation between the discrete energy levels is larger than the thermal energy, a quantum dot (QD) may form between them [2]–[5].

Here, we report on our investigations of the Coulomb blockade dominated conduction behaviour of such CNT based QDs. Apart from conventional transport experiments we show that surface acoustic waves (SAW) can be exploited to drive a quantized current through CNT QDs.

On a piezoelectric substrate, a SAW is accompanied by large electric fields, propagating at the speed of sound [6]. Due to the acoustoelectric effect, momentum from the wave is transferred to mobile charges in the CNT, driving an acoustoelectric current through the nanotube [7, 8]. Moreover, the SAW electric fields also modulate the metal–CNT potential barriers at a time scale of the SAW frequency, especially if the size of the QD matches half of the SAW wavelength. In this case, the 'source' potential barrier between metal and CNT is lowered at a given point in time, whereas at the same time the 'drain' barrier is raised by the SAW potential. Hence, an electron

can tunnel into the QD from the source. Half a SAW period later, the situation reverses and the electron tunnels out of the QD. This particular situation leads to a quantized acoustoelectric current with exactly one electron per SAW cycle. Such turnstile devices are presently being investigated with the aim of developing a new current standard in semiconductor and CNT QDs [7, 9].

2. Preparation

Two samples (in the following denoted as sample A and B) were prepared on lithium-niobate-substrate ($LiNbO_3$ 128-Y-cut-X-propagation) by standard electron-beam lithography. The contacts on sample A were made of 5 nm titanium and 25 nm gold, on sample B of 5 nm titanium and 25 nm aluminium. On all samples two different interdigital transducers (IDT) for SAW generation [10] were processed. The IDT_1 having a wavelength of $\lambda_1 = 28\,\mu m$ ($f_1 = 128\,MHz$) was employed for tube-alignment [11], whereas the second transducer (IDT_2) served to generate a SAW of $\lambda_2 = 2\,\mu m$ ($f_2 = 2\,GHz$) for the acoustoelectric experiments. To match the commensurate condition pointed out above, the source (S) and drain (D) distance between the contacts to the CNT was adjusted to approximately half this wavelength (see below).

Following the CNT alignment procedure in Strobl *et al* [11], a single drop of CNTs ($V \approx 0.4\,\mu L$) suspended in deionized water and sodium-dodecylsulfate (SDS) was applied to a capillary gap between the $LiNbO_3$ substrate and a cover slide. For about 20 min, a radio frequency signal of $P = 16\,dBm$ power and the respective IDT resonant frequency f_1 was applied to the low frequency IDT_1 in order to launch a SAW with large amplitude. This large amplitude SAW is used to successfully align the CNT with respect to the contact pattern. Finally, the samples were rinsed in deionized water for 2 min and were dried with nitrogen gas.

After alignment the samples were inspected by a scanning electron microscope (SEM), employing a temporary thin SiO_x/Al coating. Aluminium was chemically removed after inspection. The result of this SEM investigation is shown in figure 1.

The dominating alignment angle between CNT and metal contact turned out to be close to $90°$, as expected for a metallic environment and in contrast to the alignment on a free surface [11]. For the case of a metalized surface the piezoelectric SAW fields are efficiently screened leaving a large field gradient directly at the edges of the metal electrodes. In this sense, the SAW driven alignment procedure is similar to the dielectrophoresis process for CNT alignment presented in [12].
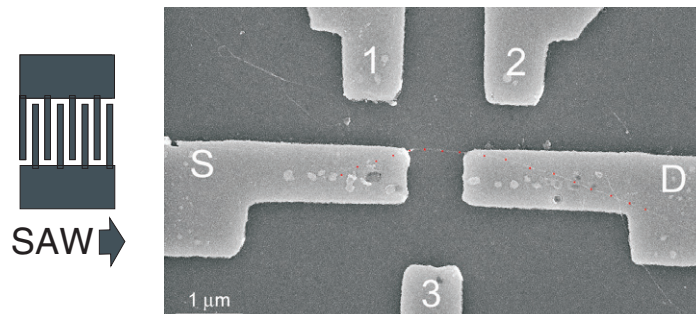
3. Measurements

3.1. Coulomb blockade oscillations

The lithographically defined contact pattern of sample A is shown in figure 2. S and D denote the source and drain contacts, three additional gate electrodes are numbered 1, 2 and 3. The SD distance of $d_{SD} = 0.9\,\mu m$ is bridged by a single CNT, having a length of about $l_{CNT} = 6\,\mu m$.[4]

---

[4] It cannot be excluded that the CNT consists of a small bundle. However, the transport characteristics are dominated by a single metallic CNT.
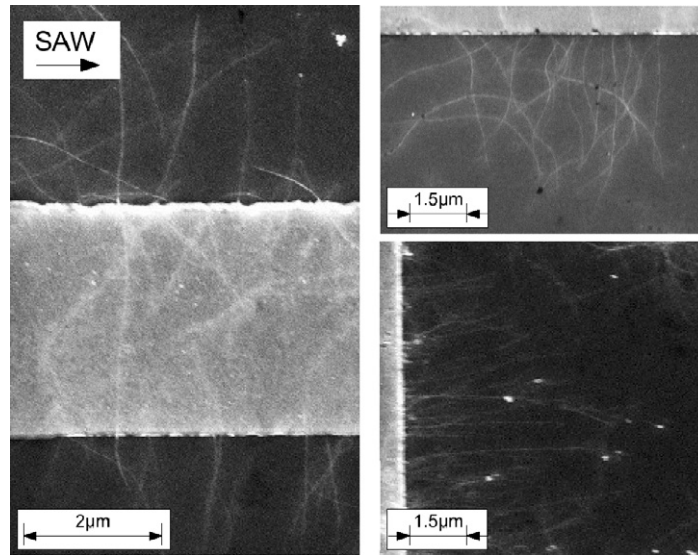
Figure 1. SEM images of electrodes and CNTs after alignment. The electric field of the SAW is shortened at the conducting leads and the resulting electric field gradient rotates the CNTs perpendicular to the metallic borders.

Figure 2. Typical structure used for transport measurements. Source (S) and drain (D) electrodes are contacted by a CNT. The gate electrodes are labelled with 1, 2 and 3 and only gate 3 is used in order to control the electronic states in the CNT. The sketched IDT on the left is not to scale but to clarify its position relative to the CNT device.

In general, the existence of a coulomb blockade can be proved by two preconditions. Firstly, the resistance of the system must hold the relation $R \gg (h/e^2) \approx 25.9 \, \text{k}\Omega$. Secondly, the charging energy U of the dot has to be larger than the thermal energy $E_{\text{th}} = k_{\text{B}}T \, (\approx 0.36 \, \text{meV}$ at liquid helium temperature).

Transport measurements at room temperature exhibit non-ohmic and non-symmetric I–V-characteristics for positive and negative bias values (blue curve in figure 3). The slope of the I–V curve corresponds to the CNT conductance, its reciprocal to the resistance, respectively. At positive source–drain bias ($V_{\text{SD}} > 0$) we obtain $R_{\text{SD}}^+ = 1.3 \, \text{M}\Omega$ and for negative $V_{\text{SD}} < 0$ the resistance is $R_{\text{SD}}^- = 2 \, \text{M}\Omega$. Nevertheless, because there is no indication of a gate bias dependence
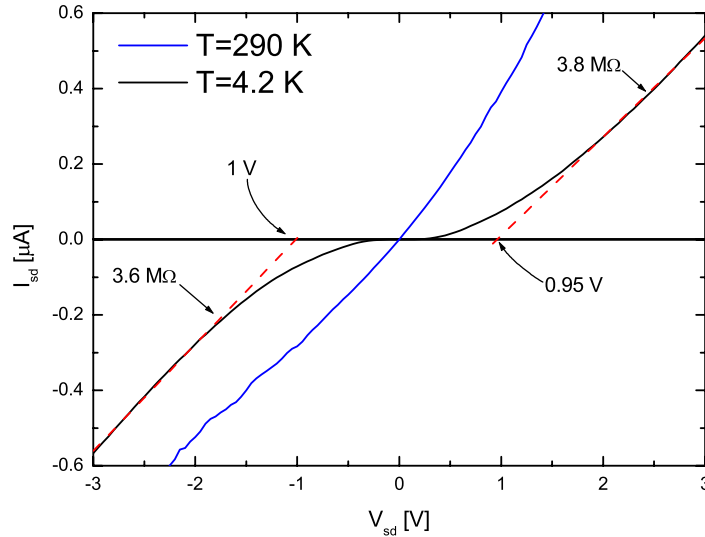
Figure 3. Typical *IV*-measurement of a CNT contact at room temperature (blue) and at $T = 4.2\,\mathrm{K}$ (black) showing significant differences. Whereas the room temperature curve also shows conductivity near zero bias, the low temperature measurement exhibits a blockade region without conductivity caused by a contact barrier. The first derivative (red) of the linear parts of this curve delivers the resistance of the contact and an estimation of the barrier height at $T = 0$.

on the *I–V* curve, we thus assume the CNT to be in a metallic state [13]. Asymmetries in the *I–V*-measurements can be caused by the differing quality of source and drain contacts. While cooling the sample down to $T = 4.2\,\mathrm{K}$ the contact barriers gain influence, which due to the lack of thermal energy cannot be overcome by the electrons. By application of a finite source–drain voltage V_{SD}, however, the barriers can be passed leading to a finite source–drain current (I_{SD}) above a certain bias threshold. This behaviour is reflected in the typical *I–V* curve as shown in figure 3 (black curve). Only for $|V_{\mathrm{SD}}| > 0.3\,V$, a measurable current is observed. For larger V_{SD}, the *I–V* curve becomes linear again and reveals resistances $R_{\mathrm{SD}}^{+} = 3.8\,\mathrm{M\Omega}$ and $R_{\mathrm{SD}}^{-} = 3.6\,\mathrm{M\Omega}$, respectively. From the blocked conductivity region in figure 3, we estimate the finite contact barrier height Φ to approx. $1\,\mathrm{eV}$ at $T = 0\,\mathrm{K}$. Hence, the first prerequisite for the existence of a Coulomb blockade is met.

An estimation of the charging energy of CNT QDs has been reported by Nygard [13]. The approximated charging energy U is mainly dependent on the length L of the CNT between source and drain contact and the dielectric function ε_{r} of the surrounding material:

$$U = \frac{e^2}{\varepsilon_0 \varepsilon_{\mathrm{r}} L}. \tag{1}$$

For the contacts presented here the CNTs are surrounded by LiNbO$_3$ (bottom) and SiO$_x$ (top) due to the fabrication process as described above. The resulting average dielectric function is therefore:

$$\varepsilon_{\mathrm{r}} = \frac{65(\mathrm{LiNbO_3}) + 4(\mathrm{SiO_2})}{2} = 34.5. \tag{2}$$
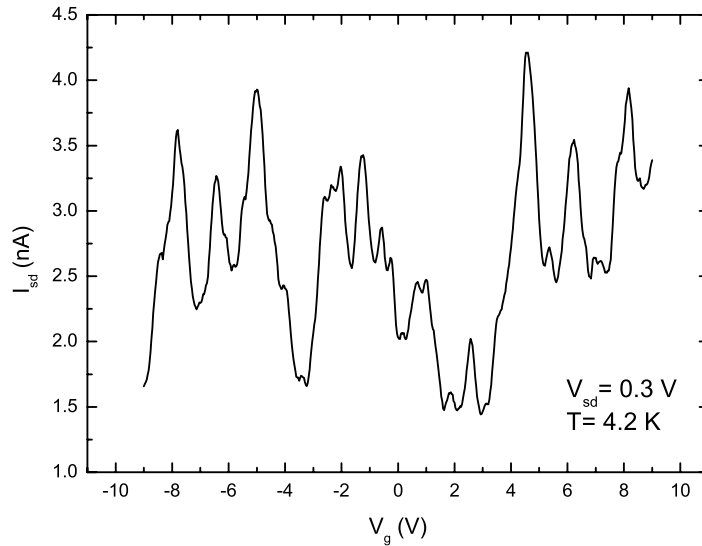
Figure 4. Coulomb oscillations for an applied source–drain voltage of $V_{sd} = 0.3\,\text{V}$ with a periodicity of about $\Delta V_g = 1.8\,\text{V}$. The gate voltage was applied at gate electrode 3.

For the contacted CNTs with a length of $L = 0.9\,\mu\text{m}$ this approximation results in a charging energy of $U = 0.6\,\text{meV}$. This is about double the thermal energy of the electrons at liquid helium temperature and therefore also the second precondition for Coulomb blockade should be fulfilled.

The measured source–drain current I_{SD} as a function of gate voltage V_G at low temperature and a finite source–drain voltage of $V_{sd} = 0.3\,\text{V}$ is presented in figure 4. This measurement was accomplished using only gate 3. The other gate electrodes remained unbiased. In agreement with the predictions made above Coulomb oscillations with an averaged periodicity of $\Delta V_g = 1.8\,\text{V}$ have been detected. But in contrast to the results of [2]–[5] the oscillations are not strictly periodic and also the current does not drop down to zero in between the peaks. Therefore there are some deviations from a well defined CNT single QD system. We assume that our fabrication process has created defects within the CNT leading to a few QDs in series. A charge transport through QDs in series within a single CNT results in an aperiodic oscillation pattern and a non-closing gap in the Coulomb blockade 'diamonds' [14]–[16] as detected experimentally (see figure 4). Therefore we have a system with Coulomb blockade in CNTs but a system consisting of a few QDs in series. This splitting of our contacted CNT into several dots leads to a decrease of each QD length and therefore (taking equation (1) into account) causes an increase of each charging energy. This finally leads to this non-closing gap.

The splitting of the CNT could also explain the discrepancy between the estimated charging energy $U = 0.6\,\text{meV}$ using equation (1) and the detected current blockade for $V_{sd} < 0.3\,\text{eV}$. Equation (1) is just an order of magnitude estimate for U and leads, due to the splitting into shorter QDs, to an underestimation of the charging energy of the system.

3.2. Acoustoelectric effects

We now turn to the SAW induced acoustoelectric currents through the CNT based QD system as described and characterized above. A SAW from IDT_2 is launched towards and along the
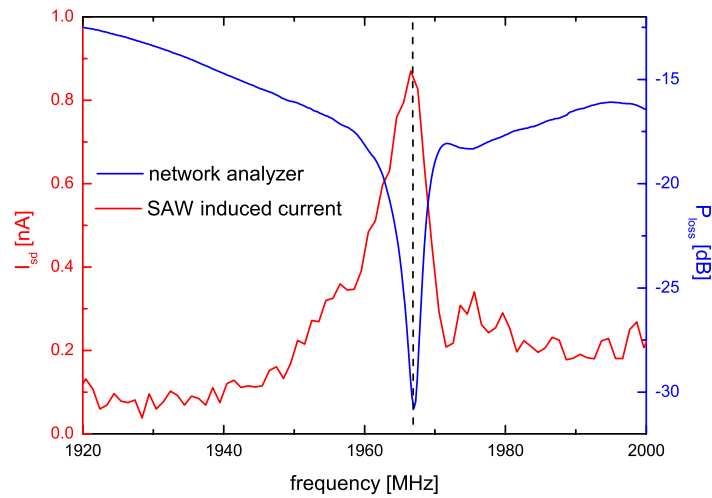
Figure 5. The red graph depicts SAW-induced current at frequencies between 1920 and 2000 MHz with a SAW amplitude of 13 dBm. The current maximum is reached at 1967 MHz which is the resonant frequency of the relevant IDT as the insertion loss measurement (blue) shows.

CNT attached to the source and drain contacts (see figure 2). The piezoelectric fields of the SAW transfer momentum to the charge carriers [17], resulting in a finite current through the CNT. As a first proof of such a SAW induced acoustoelectric current, we present a frequency dependent measurement of the SD current as a function of the frequency f_2 at the transducer IDT_2. The IDT has a resonance frequency of about $f_{res,2} = 1967$ MHz, corresponding to a SAW wavelength of $\lambda_{SAW,2} = 2\,\mu$m. The result is shown in figure 5. Here we depict the IDT frequency response (insertion loss, measured using a vector impedance analyser) together with the current as measured across source and drain at zero DC bias. Clearly, the current exhibits a resonance at exactly the same frequency as the IDT response, indicating an acoustoelectric origin.

3.3. Quantized current

SAW driven quantized acoustoelectric current has been observed in GaAs/AlGaAs based QDs [9]. Here, we wish to report on our observation that such quantized acoustoelectric current can also be achieved in CNT based QDs. Due to their small diameter single walled CNTs offer the opportunity to realize QDs with extraordinarily large charging energies [18]. In figure 7, we present measurements of the acoustoelectric current as a function of radio frequency (RF) power for a device (sample B) similar to the one shown in figure 2. Even for zero source–drain bias we measure a source–drain current under SAW application. This current reaches a plateau ($I_p = 322$ pA) at a RF power of $P = 11$ dBm for the resonant SAW frequency of this IDT_2 of $f_{res,2} = 2008$ MHz of this device. At larger RF power levels than $P = 13$ dBm there is a further increase in acoustoelectric current caused by a larger SAW amplitude. Due to problems with the measurement set-up this CNT device was destroyed before detailed gate voltage dependencies or source–drain voltage dependencies on the acoustoelectric current could be made. But before the sample was damaged a frequency variation was made and the result is presented as an inset of figure 6. Frequencies inside the passband of IDT_2 from 2006 to 2010 MHz have been used
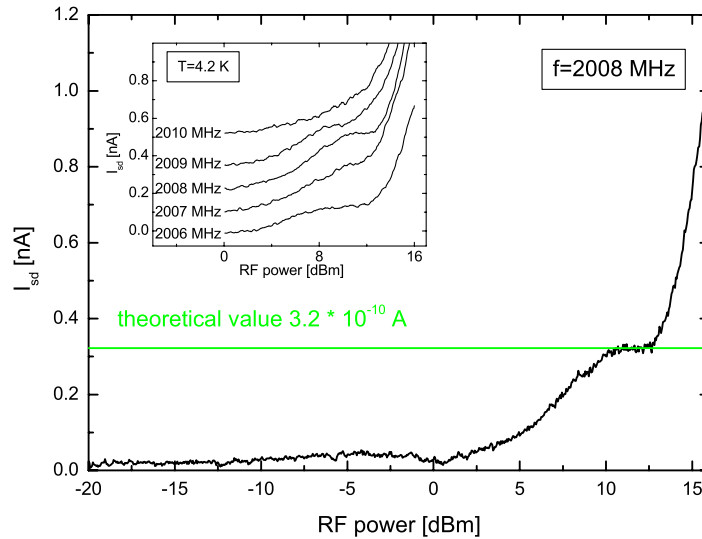
Figure 6. At $T = 4.2\,\mathrm{K}$ and zero source–drain bias the SAW driven current through the CNT QD is measured varying the SAW amplitude. The respective resonance frequency is $f_{\mathrm{res},2} = 2008\,\mathrm{MHz}$. The current shows a plateau exactly at the theoretical calculated value of $3.22 \cdot 10^{-10}\,\mathrm{A}$. Inset: acoustoelectric current versus RF power for different SAW frequencies inside the IDT's passband. The curves have been shifted by $100\,\mathrm{pA}$ for clarity.

and a strong dependency of the quantization accuracy on the applied RF frequency is exhibited. This is in accordance with measurements obtained with GaAs/AlGaAs based devices [19]. The presented explanation is a change of the position of the SAW amplitude's minima and maxima for frequency variation due to an superimposed standing wave pattern caused by a part reflection of the SAW at other IDTs on the sample. For this particular sample no detailed measurements of the charging energy of the CNT QD could be made (also due to the mentioned problems with the measurement set-up), but we estimate it to be of the same order as the one for sample A based on the same lithographically defined dimensions and the same CNT source.

The mechanism of SAW mediated single electron transport in CNT QDs is schematically shown in the cartoon presented in figure 7. A CNT is contacted by the metallic source and drain leads and the developing tunnlling barriers define a CNT QD in between. A SAW is a mechanical surface wave which in the case of piezoelectric substrates is also accompanied by an electric field of the same wavelength. This piezoelectric field is the driving force of this CNT turnstile device, if the SAW wavelength has been set to approximately twice the length of the contacted CNT. At $t = t_0$, the dynamic SAW potential minimum lowers the entrance tunnelling barrier and a single electron can enter the CNT QD. Coulomb interaction leads to a repulsion of further electrons and therefore determines the width of the current plateau. For the same moment in time, the piezoelectric local maximum is at the position of the drain tunnel barrier. The potential height of this barrier is therefore raised, preventing co-tunnelling of the electron. Half a wavecycle later (in this case $t_1 = t_0 + 1\,\mathrm{ns}$), the piezoelectric SAW potential minimum has reached the exit tunnel barrier and the single electron can leave the CNT QD. The entrance tunnel barrier is raised and no further electron can enter the CNT QD. Hence, for each SAW cycle one single electron is
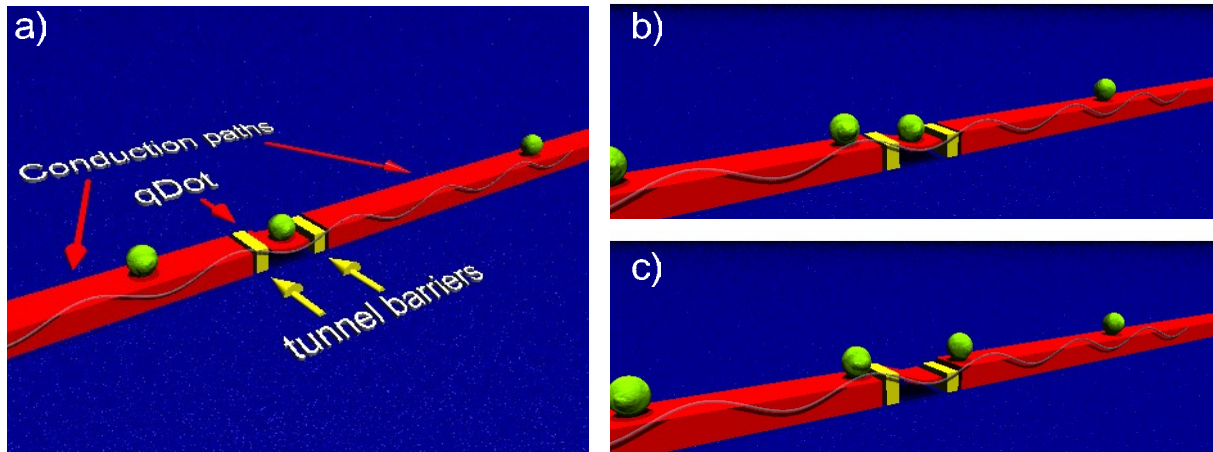
Figure 7. Snapshots from a cartoon of the SAW driven single electron transport through a QD. The complete animation is available online.

transported through the device leading to a quantized current

$$I = ef = 2.008 \times 10^9 \, \text{Hz} \times 1.6 \times 10^{-19} \, \text{C} = 3.217 \times 10^{-10} \, \text{A}. \tag{3}$$

The measured current plateau at $I_\text{p} = 322$ pA agrees very well with the one theoretically expected from this relation. This precise quantization is on the one hand surprising due to the fact that there are several QDs in series in the present system that should affect the turnstile mechanism. But on the other hand the main transport limiting tunnel barriers are the metal electrode/CNT contacts and therefore the SAW induced modulation of these dominating tunnel barriers in an alternating way leads to the current quantization.

4. Summary

In conclusion we have presented measurements on CNTs that were confined to QDs by the contacting mechanism. Due to the length of the contacted CNT being less than a micrometre and a high two-terminal resistance, the assumption of dimensionality reduction to QDs is justified. This has been verified by the presented Coulomb blockade measurements. Additionally these investigations exhibit the existence of a few unintentional QDs within the contacted CNT, probably created during the sample fabrication process. Applying a SAW with finite amplitude to such a CNT QD system results in an acoustoelectric current transport. Adjusting the SAW wavelength to be approximately twice the length of the contacted CNT leads to a quantization of the current which can be explained by a turnstile-like transport mechanism. The device performance and therefore the quantization accuracy can be enhanced by improving the metal electrode/CNT contacts that would lead to a better defined CNT QD and would therefore also allow detailed gate voltage and source–drain voltage dependency measurements.

IOP Institute of Physics **Φ** DEUTSCHE PHYSIKALISCHE GESELLSCHAFT

References

[1] Iijima S 1991 *Nature* **354** 56–8
[2] Ishibashi K, Ida T, Suzuki M, Tsukagoshi K and Aoyag Y 2000 *Japan J. Appl. Phys.* **39** 7053–7
[3] Jarillo-Herrero P, Sapmaz S, Dekker C, Kouwenhoven L P and van der Zant H S J 2004 *Nature* **429** 389
[4] Park J and McEuen P L 2001 *Appl. Phys. Lett.* **79** 1363
[5] Nygard J and Cobden D H 2001 *Appl. Phys. Lett.* **79** 4216
[6] Wixforth A, Kotthaus J P and Weimann G 1986 *Phys. Rev. Lett.* **56** 2104
[7] Ebbecke J, Strobl C J and Wixforth A 2004 *Phys. Rev.* B **70** 233401
[8] Leek P J, Buitlaar M R, Talyanskii V I, Smith C G, Anderson D, Jones G A, Wei J and Cobden D H 2005 *Phys. Rev. Lett.* **95** 256802
[9] Ebbecke J, Fletcher N E, Janssen T J B M, Ahlers F J, Pepper M, Beere H E and Richie D A 2004 *Appl. Phys. Lett.* **84** 4319
[10] Farnell G W 1977 *Surface Wave Filters* (New York: Wiley)
[11] Strobl C J, Schäfein C, Beierlein U, Ebbecke J and Wixforth A 2004 *Appl. Phys. Lett.* **85** 1427–9
[12] Krupke R, Hennrich F, Weber H B, Kappes M M and Löhneysen H v 2003 *Nano Lett.* **3** 1019
[13] Nygard J, Cobden D H, Bockrath M, McEuen P L and Lindelof P E 1999 *Appl. Phys.* A **69** 297–304
[14] Babic B, Iqbal M and Schönenberger C 2003 *Nanotechnology* **14** 327
[15] Moriyama S, Toratani K, Tsuya D, Suzuki M, Aoyagi Y and Ishibashi K 2004 *Physica* E **24** 46
[16] Zhou Z, Jin R, Eres G, Subedi A and Mandrus D 2006 *Appl. Phys. Lett.* **89** 133124
[17] Weinreich G 1956 *Phys. Rev.* **104** 321
[18] Maehashi K, Ozaki H, Ohno Y, Inoue K, Matsumoto K, Seki S and Tagawa S 2007 *Appl. Phys. Lett.* **90** 023103
[19] Talyanskii V I, Shilton J M, Pepper M, Smith C G, Ford C J B, Linfield E H, Ritchie D A and Jones G A C 1997 *Phys. Rev.* B **56** 15180